Energies **2015**, *8*, 6528-6542; doi:10.3390/en8076528

OPEN ACCESS

energies

ISSN 1996-1073

www.mdpi.com/journal/energies

Article

Nonlinear Passive Control of a Wave Energy Converter Subject to Constraints in Irregular Waves

Liguo Wang * and Jan Isberg

Department of Engineering Sciences, Swedish Centre for Renewable Electric Energy Conversion, Division of Electricity, the Ångström Laboratory, Uppsala University, P.O. Box 534, 75121 Uppsala, Sweden; E-Mail: jan.isberg@angstrom.uu.se

* Author to whom correspondence should be addressed; E-Mail: liguo.wang@angstrom.uu.se; Tel.: +46-18-471-5908.

Academic Editor: Jens Peter Kofoed

Received: 17 April 2015 / Accepted: 18 June 2015 / Published: 29 June 2015

Abstract: This paper investigates a passive control method of a point absorbing wave energy converter by considering the displacement and velocity constraints under irregular waves in the time domain. A linear generator is used as a power take-off unit, and the equivalent damping force is optimized to improve the power production of the wave energy converter. The results from nonlinear and linear passive control methods are compared, and indicate that the nonlinear passive control method leads to the excitation force in phase with the velocity of the converter that can significantly improve the energy production of the converter.

Keywords: wave energy converter; power take off; passive control; load control; irregular waves; time domain

1. Introduction

Wave energy is the transport of power by ocean surface waves, and it has high availability, density and good predictability compared to other renewable sources. A variety of technologies for converting wave energy to electricity have been developed in the past decades [1–5]. This paper focus on a wave energy converter (WEC) concept developed at the Swedish Centre for Renewable Electric Energy Conversion at Uppsala University [6–8]. As shown in Figure 1 [9], the WEC contains two main parts, a floating buoy and a submerged linear generator. The buoy captures the energy from the ocean waves.

It has a small radius compared to the wave length, and thus belongs to the point absorber category. The linear generator plays the role of power take-off (PTO) system, and is connected to the buoy via a rope. The motion of the buoy drives the translator to move up and down, thereby converting mechanical energy into electrical energy. This WEC concept has been validated by theory and extensive real sea trials [9,10].

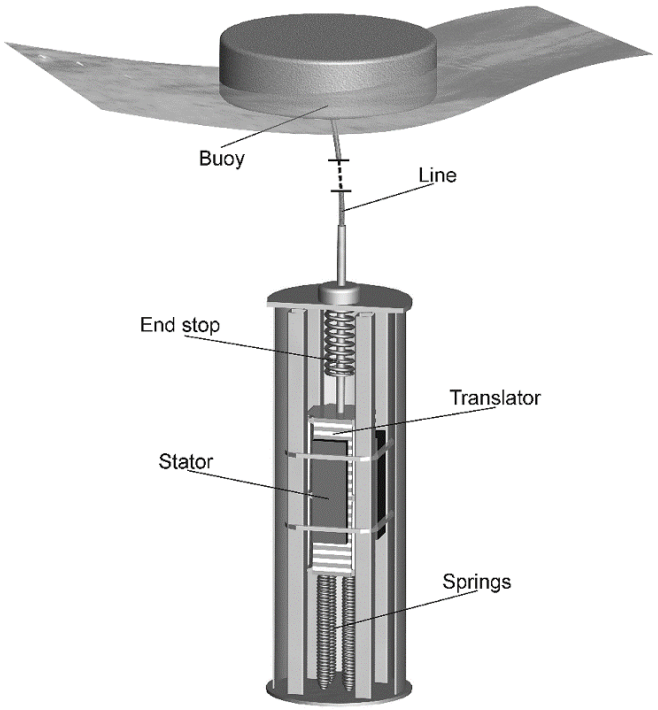

Figure 1. WEC concept developed at Uppsala University. No springs are present for the L12 version and WEC model in this paper.

Early studies indicate how the power output of the WEC is influenced by the sea state, buoy characteristics and PTO damping [11–13]. The first is given by the chosen location, but the other two can be altered and optimized in the mechanical design and dimensioning of the buoy and the choice of generator type and load connection. To optimize the PTO damping, both mechanical and electrical damping control strategies can be implemented with or without considering the restricted displacement amplitude of the WEC [14–16].

In the mechanical control, some mechanical mechanisms are implemented to adjust the PTO force and optimize the velocity of the PTO's moving parts. Latching control [17,18] and clutching control [19] are two representative methods for this. Latching control blocks and drops the buoy at suitable time instants to adjust the excitation force in phase with the velocity of the buoy [20]. Clutching control couples and decouples the machinery to let the buoy move freely in periods. In that way, the optimal phase condition can be obtained without reactive power flow in the machinery.

While the mechanical control must be operated near the PTO side in the ocean, the operation of the electrical damping control can be arranged on shore since the electricity produced by the PTO can be transmitted over a long distance to the electrical circuits on land, which is more convenient and economical. In the electrical damping control, the values of the electrical components, such as a resistor or capacitor, are adjusted to improve the performance of the WEC. The PTO force $F_{PTO}(t)$ can be

decomposed into two components, one is about the velocity $\dot{z}(t)$ and another is about the displacement $z(t)$, viz. $F_{PTO}(t) = -C\dot{z}(t) - Kz(t)$, where C and K are coefficients that should be nonnegative.

Two main strategies for the electrical control are passive control [21,22] and active control [23–25]. For passive control, the reactive component of the PTO is set to zero, and only C is controlled. The active control necessitates tuning of both K and C, which requires bidirectional power flow between the PTO and device. This leads to a large energy exchange [26]. Furthermore, the reactive control involves high oscillating excursion, which is unacceptable for a linear generator. There are two main advantages for passive control. One is that it can be implemented in a simple way, and another is that the passive control can significantly decrease the ratio of peak power to mean power produced by the WEC [27]. This paper focuses on the passive control method for the WEC.

For the passive control, different time scales can be applied for the damping tuning. The simplest case is that the damping coefficient C is constant and will never be tuned, which corresponds to linear passive control (LPC). Then the PTO force will be proportional to the velocity. However, the sea state is not regular and varies with time. Therefore, it is necessary to tune C with time to maximize the power absorbed from the ocean waves. In this case, the passive control is nonlinear. The control diagram is shown in Figure 2. It should be noted that the implementation of these control schemes are highly dependent on the controllers, which are not discussed in this paper.

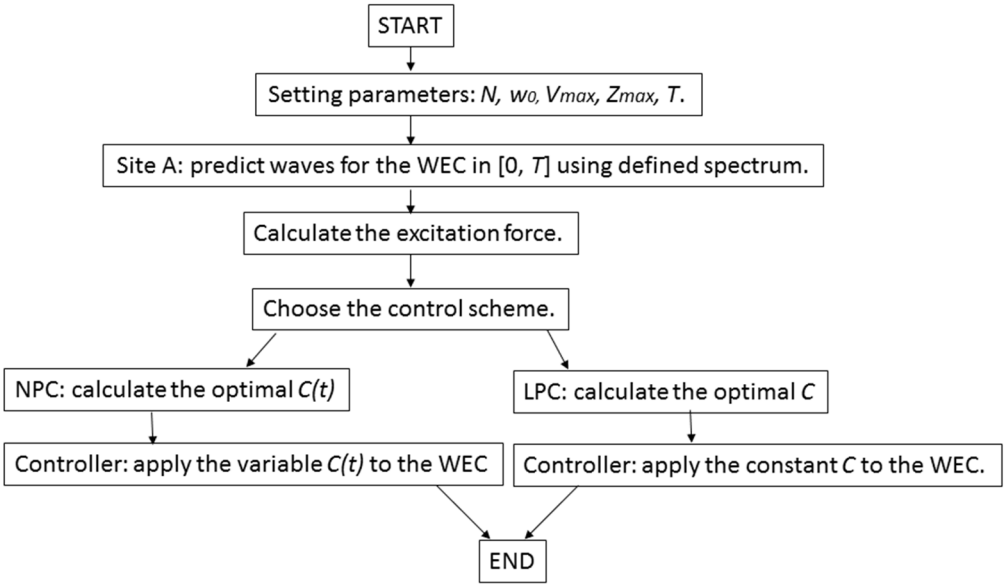

Figure 2. Control diagram for the WEC.

Some theoretical and experimental studies of passive control have been investigated. Budal & Falnes first showed that the absorbed energy can be converted into electrical energy by a generator and this performance can be improved by adjustable load resistance [4]. Later, Hals compared the passive control method with other methods under regular and irregular waves, and results show that the passive control has lower peak-mean power ratio, corresponding to a smoother power fluctuation [27]. In another study [21], assuming the damping coefficient tuned at a time scale ranging from hourly to annually, the passive control method is used to evaluate power output of the Oregon coast for the whole year, where the power is calculated in the frequency domain. Furthermore, the time domain study is needed if the constraints are considered. In recent studies [28,29], Bacelli *et al.* studied the maximization of energy

production of WECs under displacement constraint based on the approximation of the motion of the WEC and of the PTO force by means of a combination of basis functions.

In this paper, using the same basis functions, the motion of the WEC and the PTO force are expanded in terms of truncated Fourier series. The motion constraints and the sign of the damping coefficient are considered in the solution. The damping coefficients are tuned with time under the irregular waves to maximize the mean power within a fixed time horizon. Therefore our approach belongs to the category of nonlinear passive control (NPC). It should be noted that the damping coefficients are required to be nonnegative here, something that is usually ignored by other investigators. This corresponds to the physical characteristics of a resistor in electrical circuits, which means its value must be nonnegative, and the resistor will always consume power no matter whether the voltage is positive or negative. A displacement constraint is necessary for the linear generator, since it plays a role in protecting the hull of the generator from being struck by the translator. Reference [30] indicates that the induced peak voltage of the generator and velocity amplitude have a correlation, and even coincide, so that the peak voltage can be limited by introducing a constraint on the velocity amplitude. The influence of the displacement constraint and the velocity constraint to the performance of the WEC under regular waves has been investigated in our previous work [31].

The structure of this paper is as follows. In Section 2, the dynamic model of the point absorber WEC is established, and the resulting optimization problem is presented in a standard format with the cost function and constraints. In Section 3, simulation results are demonstrated and discussed. Finally, the paper is concluded in Section 4.

2. Methodology

2.1. Wave Model

In order to evaluate the performance of the WEC in real seas, the analysis of the WEC under irregular waves is necessary. For ocean waves driven by wind, the superposition theory can be used to describe the irregular waves under the assumption that the wave heights are small compared to the wave length. Then the irregular wave elevation can be created by summing regular wave components of small height, random phase, and different frequencies [32], as follows:

$$\xi(t) = \sum_{i=1}^{N} \alpha_i \cos(w_i t + \Theta_i) \tag{1}$$

where $w_i = i \times w_0$, Θ_i, α_i are the angular frequency, phase, amplitude of the *i*th harmonic wave respectively, and w_0 is the fundamental angular frequency from:

$$w_0 = w_{\max}/N \tag{2}$$

where $w_{\max}$ is the maximum frequency component present in the spectrum and N is the number of wave components.

The wave amplitude can be derived from the wave spectrum $S(w)$ as:

$$\alpha_i = \sqrt{2S(w_i)dw} \tag{3}$$

where $dw = w_0$ is the wave frequency interval.

Ocean waves are produced by the wind. The faster the wind, the longer the wind blows, and the bigger the fetch over which the wind blows, the bigger the waves. To describe the ocean wave spectrum, various idealized spectra have been used. The Pierson-Moskowitz spectrum, a relatively simple spectrum, is used to describe the case where the wind blew steadily for a long time over a long fetch. If the wave spectrum is not fully developed, the JONSWAP spectrum can be used instead. Assuming a fully developed sea, a modified Pierson-Moskowitz Spectrum defined by the significant wave height and the peak wave period can be described as [33]:

$$S(w) = \frac{5\pi^4 H_s^2}{T_p^4 w^5} \exp\left(-\frac{20\pi^4}{T_p^4 w^4}\right) \tag{4}$$

where w is wave angular frequency, T_p the peak wave period, H_s the significant wave height.

The nth spectral moment can be expressed in terms of the moments of the spectral function as:

$$m_n = \int_0^\infty w^n S(w) dw \tag{5}$$

and the energy period is defined as $T_e = m_{-1}/m_0$.

2.2. WEC Model

For simplicity, only heave motion is considered here. Assuming that the fluid flow is inviscid, incompressible, and irrotational, the motion of the WEC can be expressed according to Newton's law as:

$$m\ddot{z}(t) = F_{wa}(t) + F_{PTO}(t) \tag{6}$$

where m is the total mass of the buoy and translator and $\ddot{z}$ is the vertical acceleration of the WEC. $F_{PTO}(t)$ is the PTO force. $F_{wa}(t)$ is the total wave force, which is the sum of the excitation force $F_e(t)$, the radiation force $F_r(t)$ and the hydrostatic restoring force $F_h(t)$ *i.e.*:

$$F_{wa}(t) = F_e(t) + F_h(t) + F_r(t) \tag{7}$$

The excitation force is produced by an incident wave acting on the fixed body. For regular waves, the excitation force is a harmonic function of time. For irregular waves, the excitation force can be represented as the summation of the individual force components as [32]:

$$F_e(t) = \sum_{i=1}^{N} \sigma(w_i) a_i \cos(w_i t + \varphi_i) \tag{8}$$

where $\sigma(w_i)$ and φ_i are the coefficient and phase of the excitation force under the ith harmonic wave, and can be calculated using, e.g., the commercial boundary element method solver WAMIT [34].

The radiation force is the part of the hydrodynamic force produced by oscillation of the buoy in calm water. It can be approximated by the state-space method or presented by:

$$F_r(t) = -m_\infty \ddot{z}(t) - \int_{-\infty}^{t} K(t-\tau)\dot{z}(t) d\tau \tag{9}$$

where m_∞ is the infinite-frequency limit of added mass, K the impulse response function.

The hydrostatic restoring force is proportional to the buoy displacement, and can be expressed as:

$$F_h(t) = -Sz(t) \tag{10}$$

where $S = \rho g \pi r^2$ is the hydrostatic stiffness coefficient with r being the radius of buoy, ρ the water density, and g the gravitational acceleration.

2.3. Modelling of Power Absorption under Constraints

In this paper, trigonometric functions are chosen as the basis functions, and the basis vector can be expressed as:

$$\boldsymbol{L} = [\cos(w_0 t), \sin(w_0 t), \cos(2w_0 t), \sin(2w_0 t), \ldots, \cos(Nw_0 t), \sin(Nw_0 t)]^T \tag{11}$$

The velocity of the WEC can be approximated by the Fourier series, and then expressed in terms of the basis vectors as:

$$\dot{z}(t) \cong \sum_{n=1}^{N} b_n \cos(nw_0 t) + c_n \sin(nw_0 t) = \boldsymbol{L}^T \boldsymbol{V} \tag{12}$$

where $\boldsymbol{V} = [b_1, c_1, b_2, c_2, \ldots\ldots, b_N, c_N]^T$, and the "$T$" superscript indicates the transpose of a vector.

For linear passive control, the PTO force can be expressed as $F_{PTO}(t) = -C\boldsymbol{L}^T\boldsymbol{V}$, where the damping coefficient C is a constant scalar. For nonlinear passive control, the damping coefficient varies with time, and the optimal values can be derived if the optimal velocity and PTO force are known. The PTO force in the nonlinear case can be expressed as:

$$F_{PTO}(t) \cong \sum_{n=1}^{N} p_{an} \cos(nw_0 t) + p_{bn} \sin(nw_0 t) = \boldsymbol{L}^T \boldsymbol{P} \tag{13}$$

where $\boldsymbol{P} = [p_{a1}, p_{b1}, p_{a2}, p_{b2}, \ldots\ldots, p_{aN}, p_{bN}]^T$. The excitation force can be expressed as $F_e(t) = \boldsymbol{L}^T \boldsymbol{F}$, where $\boldsymbol{F} = [F_{a1}, F_{b1}, F_{a2}, F_{b2}, \ldots\ldots, F_{aN}, F_{bN}]^T$, and $F_{an} = \sigma(nw_0)\, a_n \cos(\varphi_n)$, $F_{bn} = -\sigma(nw_0)\, a_n \sin(\varphi_n)$.

Then the approximate solution to the motion equation can be found as follows (the derivation can be found in reference [28]):

$$\mathbb{H}\boldsymbol{V} = \boldsymbol{P} + \boldsymbol{F} \tag{14}$$

The matrix $\mathbb{H}$ is block diagonal and its lth block elements $\mathbb{H}^l$ can be expressed as follows with $l = 1, 2 \ldots N$:

$$\mathbb{H}^l = \begin{bmatrix} B(lw_0) & \delta \\ -\delta & B(lw_0) \end{bmatrix} \tag{15}$$

where $\delta = \big(m + A(lw_0)\big) lw_0 - S/(lw_0)$, A is the added mass, B is the damping coefficient.

Then the energy produced by the WEC in the time range [0 T] can be expressed as:

$$E = \int_0^T -F_{PTO}(t) v(t) dt \tag{16}$$

Taking a long time average, the mean power can be expressed as:

$$P_{\text{mean}} = -\frac{1}{2} \boldsymbol{P}^T \boldsymbol{V} \tag{17}$$

For the passive control, no directional power flow will occur between the device and the PTO, which is one of the differences from the reactive control. Therefore the power produced by the WEC is always nonnegative, *i.e.*, the opposite sign of the power consumed by the PTO. This is the reason for the negative sign in Equations (16) and (17).

Two motion constraints are considered here, *viz.* the displacement constraint and the velocity constraint. The displacement constraint implies that the displacement of the buoy at time t must not exceed a limiting value, which can be expressed as:

$$|z(t)| \leq Z_{\max} \tag{18}$$

where $Z_{\max}$ is the limiting value of the displacement.

The velocity constraint can similarly be expressed as:

$$|\dot{z}(t)| \leq V_{\max} \tag{19}$$

where $V_{\max}$ is the limiting value of the velocity.

For a given time horizon, *i.e.*, for a constant T, the maximum energy can be found if and only if the mean power is found. Then the objective of the paper can be converted into an optimization problem: find the optimal velocity or passive damping coefficients to maximize the mean power. This can be expressed in the standard form:

$$\begin{gathered} \text{minimize } f = \boldsymbol{P}^T\boldsymbol{V} \\ \text{subject to} \begin{cases} |z(t)| \leq Z_{\max} \\ |\dot{z}(t)| \leq V_{\max} \\ C(t) \geq 0 \end{cases} \end{gathered} \tag{20}$$

where f is the cost function.

2.4. Numerical Solution and Benchmark

The damping coefficients, which are required to be nonnegative, can be considered as independent variables. This constraint can be converted into the requirement that the power produced by the WEC is always nonnegative, viz. $p(t) = -F_{PTO}(t)v(t) = C(t)v^2(t) = -\boldsymbol{L}^T(\mathbb{H}\boldsymbol{V} - \boldsymbol{F})\boldsymbol{L}^T\boldsymbol{V} \geq 0$, Equation (20) can be rewritten as follows,

$$\begin{gathered} \text{minimize } f = \boldsymbol{P}^T\boldsymbol{V} = (\mathbb{H}\boldsymbol{V} - \boldsymbol{F})^T\boldsymbol{V} \\ \text{subject to} \begin{cases} \begin{bmatrix} 1 \\ -1 \end{bmatrix} \boldsymbol{Y}^T\boldsymbol{V} \leq \begin{bmatrix} 1 \\ 1 \end{bmatrix} Z_{\max} \\ \begin{bmatrix} 1 \\ -1 \end{bmatrix} \boldsymbol{L}^T\boldsymbol{V} \leq \begin{bmatrix} 1 \\ 1 \end{bmatrix} V_{\max} \\ \boldsymbol{L}^T(\mathbb{H}\boldsymbol{V} - \boldsymbol{F})\boldsymbol{L}^T\boldsymbol{V} \leq 0 \end{cases} \end{gathered} \tag{21}$$

where $\boldsymbol{Y} = [Y_{a1}, Y_{b1}, Y_{a2}, Y_{b2}, \ldots\ldots, Y_{aN}, Y_{bN}]^T$, and $Y_{an} = \sin(nw_0t)/nw_0$, $Y_{bn} = -\cos(nw_0t)/nw_0$.

Equation (21) is an optimization problem for the dependent variable $\boldsymbol{V}$, and is solved using MATLAB by the active-set method. The constraints are imposed only at specified time instants $t_i = N_i \times dt$ in the range [0, T], N_i are integers starting from zero and the time step is $dt = 0.1$ s. Hydrodynamic parameters, added mass and damping, are frequency dependent and calculated using the boundary potential flow solver WAMIT. Main parameters of the WEC used in the following calculation are shown in Table 1.

The ability of the WEC for extracting power from the ocean waves can be evaluated by the capture width ratio (CWR), defined as:

$$CWR = \frac{P_{\text{mean}}}{P_{avi}D} \times 100 \tag{22}$$

where D is the diameter of the buoy. The available power P_{avi} is the total time averaged power in the incident wave train per unit crest length and can be expressed as:

$$P_{avi} = kT_eH_s^2 \tag{23}$$

where k is given in the deep water approximation as $k = \rho g^2/64\pi$.

3. Results and Discussion

3.1. Performance of the WEC in One Sea State

The motion and forces of the WEC are approximated by truncated Fourier series, therefore a proper length of the Fourier series is required in the control scheme. To study the convergence and stability of the control scheme, a sample irregular wave with a significant height of 2 m and a peak period of 5.24 s is used, as shown in Figure 3. Different values of N are used in the calculation, and the result is convergent for each value. Figure 4 indicates that the mean power increases with the value of N, and tends to stabilize when $N \geq 80$. The value $N = 100$ is used in the following calculation, and $w_0 = 0.1$ rad/s, $T = 120$ s are held constant throughout the rest of this paper.

Table 1. Main parameters of the wave energy converter (WEC).

Items	Value
Buoy radius	2.0 m
Buoy draft	1.5 m
Free stroke	1.5 m
Buoy mass	5302.0 kg
Translator mass	14.0 ton
Length of stator	2.0 m
Water depth	25.0 m

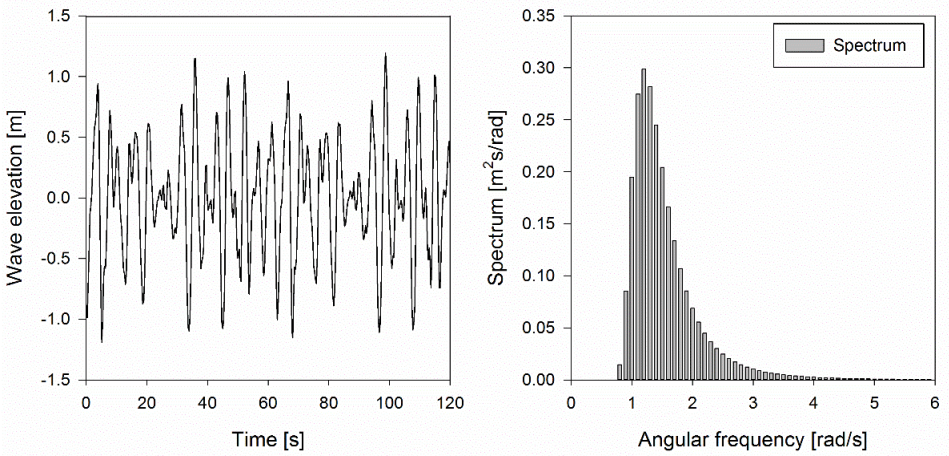

Figure 3. The sample irregular wave elevation and its spectrum. H_s = 2 m, T_p = 5.24 s.

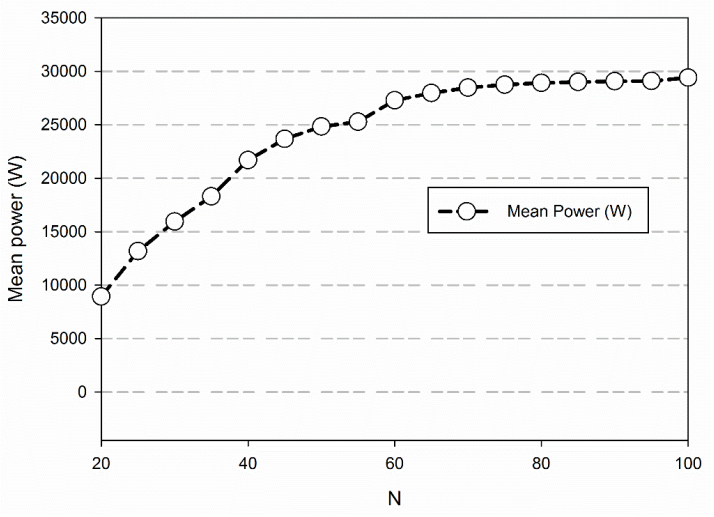

Figure 4. Mean power using different values of N. Constraints are $V_{\max}$ = 2.0 m/s, $Z_{\max}$ = 1.5 m.

The excitation force corresponding to this irregular wave and the resulting optimal motion from the NPC are shown in Figure 5. The numerical simulation results in the time domain indicate that the excitation force and the velocity of the WEC are in phase. It should be noted that the velocity of the WEC increases fast to the peak value from zero and then decreases quickly to zero, where the velocity will be kept at zero for a proper time during some instants and the corresponding displacement will be held constant. The phase shift performance is also reported in the latching control, where the displacement of the WEC is latched.

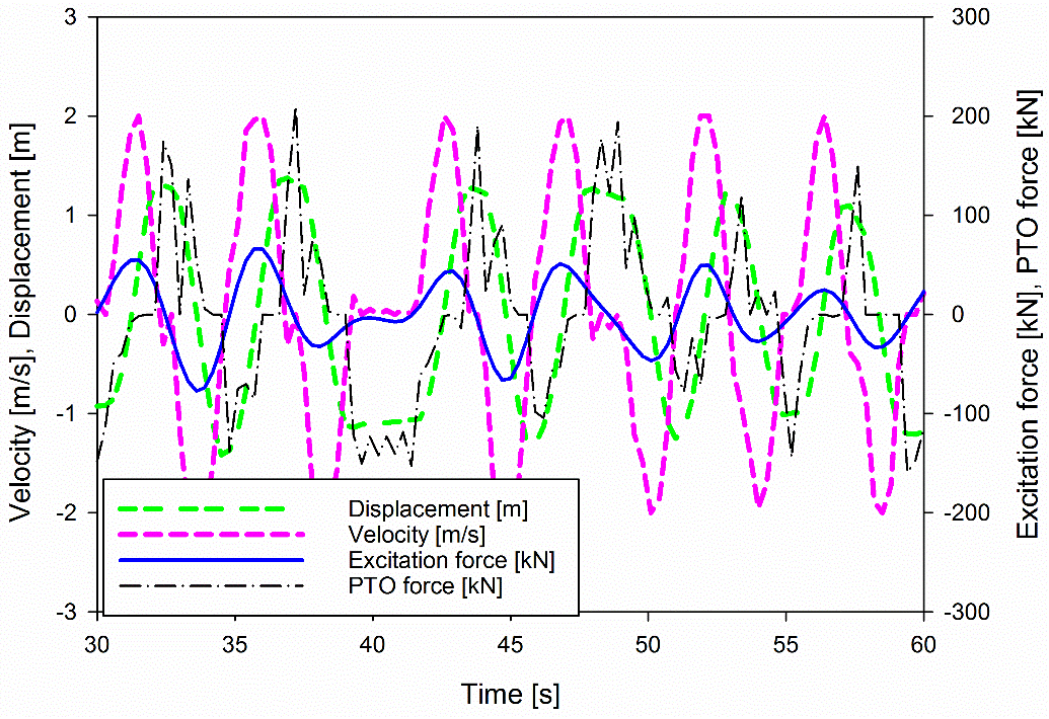

Figure 5. Velocity and excitation force of the WEC under the NPC restricting the sign of C to be nonnegative. Constraints are $V_{\max}$ = 2.0 m/s, $Z_{\max}$ = 1.5 m. Sea state is H_s = 2.0 m, T_p = 5.24 s.

In the traditional latching control, a large external force is needed to lock the motion of the WEC to maximize the absorbed power, and the optimal displacement amplitude of the translator can be very high. Using displacement constraints, the stroke will be limited to the required range and stops the translator from striking the hull of the generator. As shown in Figure 5, the displacement of the WEC does not exceed the constraint, and a large PTO force is also required in the NPC. It should be pointed out that the optimal damping coefficients are not shown directly in this figure, but can be calculated from its relationship with velocity and PTO force. The performance of the WEC under the NPC method will be evaluated in the following.

3.2. Influence of the Sign of Damping Coefficient

In the passive control, the PTO will not deliver energy back to the WEC, and all the power delivered to the PTO will be consumed by the damping part, which is the main difference compared to the reactive control. Therefore, no matter whether the buoy moves up or down, the PTO will always consume power and the power produced by the WEC will always be nonnegative. It was pointed out earlier that the sign of the damping coefficient, C, should be defined to be nonnegative in the algorithm. The instantaneous power produced by the WEC under the irregular waves shown in Figure 3 using the NPC with or without restricting the sign of damping coefficient are plotted in Figure 6. The results show that the NPC with no restriction on the sign results in negative instantaneous power. This is possible for reactive control but not possible for passive control. The mean power produced using NPC in this case is 10.5% higher than that produced by NPC with nonnegative C, as shown in Table 2. The two methods also lead to big difference in the peak power and the ratio of peak power to mean power.

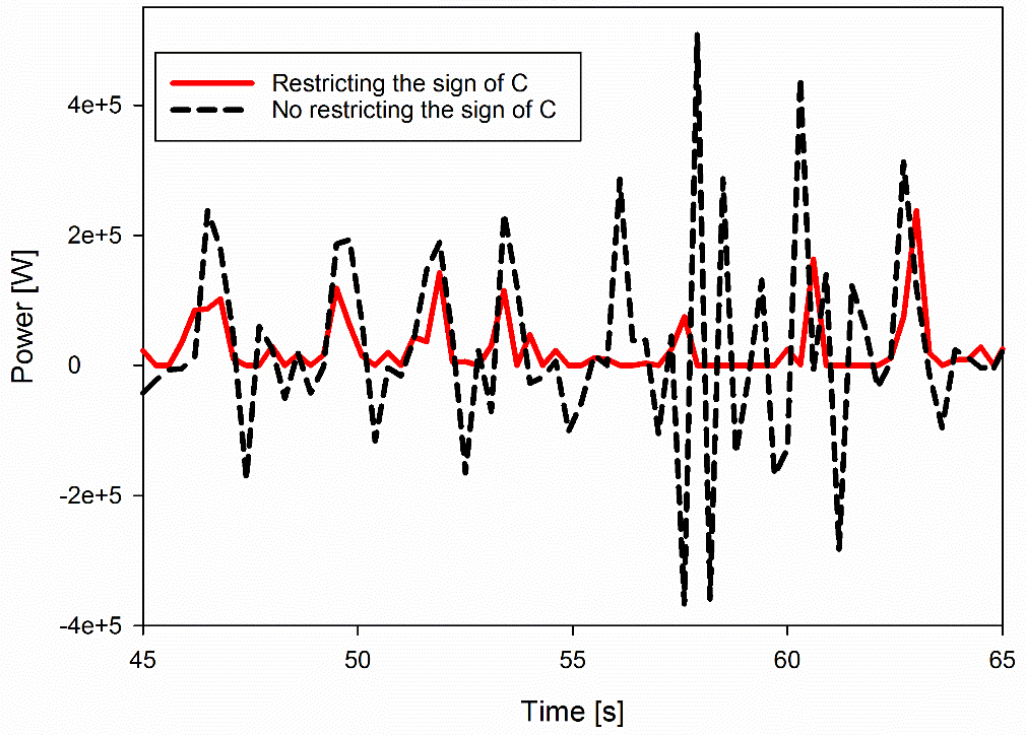

Figure 6. Instantaneous power of the WEC under NPC with or without restricting the sign of C. $V_{\max}$ = 2.0 m/s, $Z_{\max}$ = 1.5 m. H_s = 2.0 m, T_p = 5.24 s.

Table 2. Results under different requirements of the damping coefficient. H_s = 2.0 m, T_p = 5.24 s.

Item	Restricting the Sign of C to Nonnegative	No Restriction on the Sign of C
Mean power [W]	29700.0	32800.0
Peak power [W]	325400.0	702200.0
Peak/Mean	11.0	21.0

More sea states were considered to evaluate the difference between the two methods. As shown in Figure 7, the CWR decreases with the energy period in the shown range. The value is higher without the restriction of the signs of the damping coefficient. The relative difference is used to compare the results, and it can be as high as 17.9% for the energy period T_e = 7.79 s.

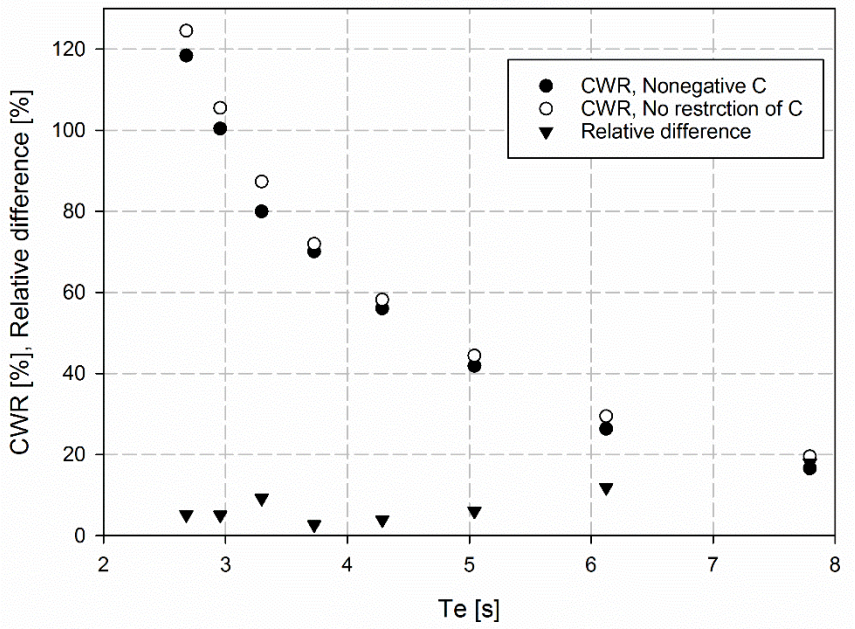

Figure 7. Capture width ratio of the WEC under NPC with or without restriction on the sign of C. The relative difference is defined as relative difference = (CWR1 − CWR2)/CWR2 × 100, where CWR1 and CWR2 are the capture width ratios with no restriction and with restriction on the sign of C, respectively. The constraints are $V_{\max}$ = 2.0 m/s, $Z_{\max}$ = 1.5 m. The significant wave height is H_s = 2.0 m.

3.3. Influence of the Constraints

Figure 8 shows the capture width ratios of the WEC under three velocity constraints and two displacement constraints with the wave energy period in the range [2s, 11s]. Results indicate that the CWR decreases with the energy period, and that it is influenced by the motion constraints. When the velocity constraint is held constant, the CWR for the same energy period increases with the value of the displacement constraint. When the displacement constraint is held constant ($Z_{\max} = 1.0$ m or $Z_{\max} = 1.5$ m), the CWR increases with the value of the velocity constraint. As shown in the cases with $Z_{\max} = 1.5$ m, the increase of the CWR under same sea state is very large when the velocity constraint is changed from 1.0 m/s to 2 m/s, while it is very small when the velocity constraint is changed from 2.0 m/s to infinity.

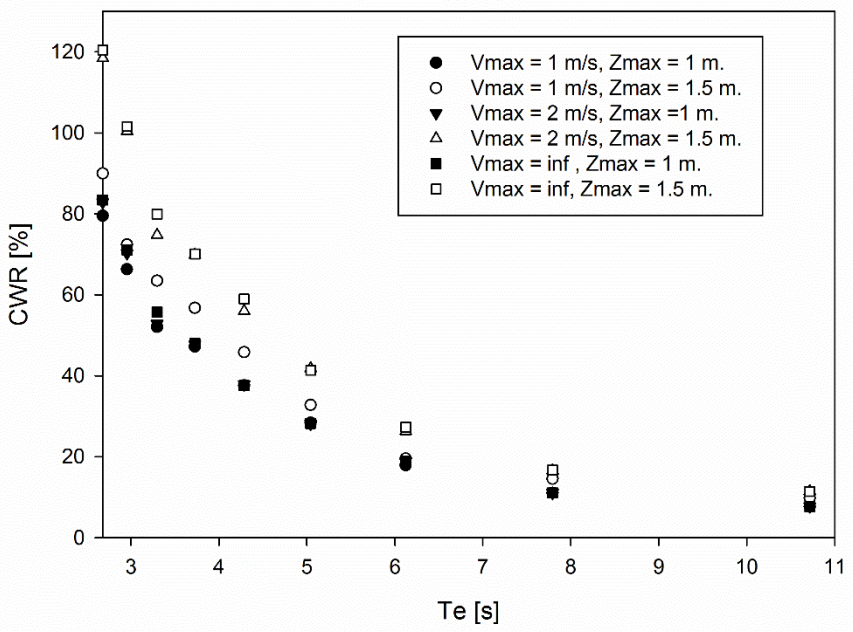

Figure 8. Performance of the WEC under NPC with different constraints. H_s = 2.0 m.

It is well known that, the displacement of the buoy needs to be increased quickly to an optimal value and held for a certain time in the latching control, which requires a fast increase and decrease of the velocity. Here, both proper values of displacement and velocity constraints are also required. If lower values are used as the constraints, less power will be produced and a large improvement in the performance of the WEC can be achieved by increasing the value of the velocity constraint or the displacement constraint. On the other hand, no improvements will be achieved by changing the velocity constraint if the velocity of the buoy is already fast enough for the corresponding displacement constraint.

3.4. Performance of the NPC under More Sea States

To evaluate the performance of the WEC under the NPC, the results from the LPC have been calculated for comparison. For the LPC, the damping coefficient is constant, and the optimal value will be chosen by the designer. Its value has a significant influence on the performance of the WEC. As shown in Figure 9a, the CWR is a function of the damping coefficient [35]. The peak value of CWR for the WEC under this sea state is approximately 26.6% when the damping coefficient is 290.0 kN·s/m.

It should be pointed out that the performance of the WEC also varies with the sea states using the same constant damping coefficient. To have a better comparison, different optimum damping values are used in different sea states in the calculation of LPC, as shown in Figure 9b. The CWR using LPC decreases with the energy period. The CWR using the NPC also varies with the energy period, but its value is higher under the same sea states, which corresponds to a better performance of the WEC. The ratio between the CWRs from two methods are calculated for comparison.

As shown in Figure 9b, the ratio increases approximately from 4.5 to 6.2 with the energy period, and then decreases to 4.5, corresponding to that the CWR using the NPC is at least 4.5 times that of the LPC in the shown range of energy period.

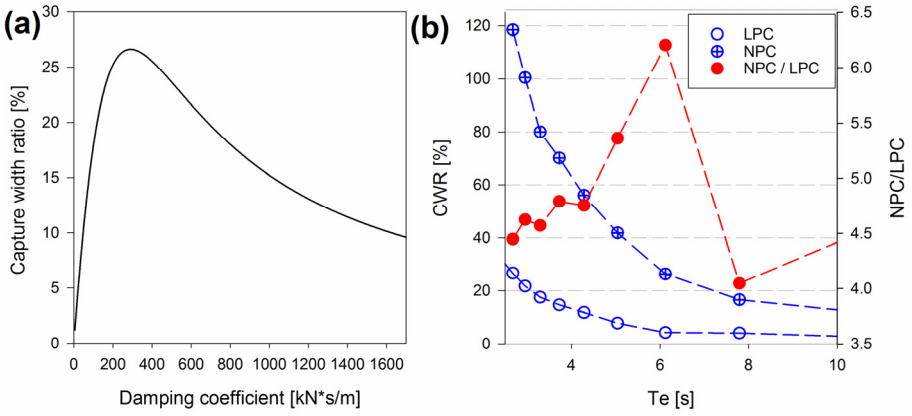

Figure 9. (**a**) Capture width ratio as a function of the damping coefficient with energy period $T_e = 2.68$ s; (**b**) The comparison of the results under NPC and LPC. NPC/LPC is the ratio between the CWRs from NPC and LPC.

4. Conclusions

In this paper, a passive control model for a point absorber wave energy converter connected to a nonlinear load has been described. A time domain simulation has been used to evaluate the performance of the wave energy converter under irregular waves considering the realistic constraints on velocity and displacement. The results indicate that the excitation force and the velocity are in phase. The performance of the WEC is sensitive to the motion constraints. The sign of the damping coefficient should be considered and requiring it to be nonnegative has a substantial influence on the results.

Compared to the classical linear passive control, the nonlinear passive control including constraints can significantly improve the performance of the WEC by more than four times in the studied range of energy period. This nonlinear passive control also enlarges the bandwidth of the wave energy converter [36].

Acknowledgments

This project was supported by the Guangzhou Elite Project of Guangzhou Government, Uppsala University, the Swedish Energy Agency and Standup for Energy.

Author Contributions

Liguo Wang coordinated the main theme of this paper and prepared the manuscript. Jan Isberg supervised this study and commented on the manuscript. Both authors read and approved the final manuscript, and contributed to the revision.

Conflicts of Interest

The authors declare no conflict of interest.

References

1. Drew, B.; Plummer, A.R.; Sahinkaya, M.N. A review of wave energy converter technology. *Proc. Inst. Mech. Eng. Part. J. Power Energy* **2009**, *223*, 887–902.

2. Falnes, J. A review of wave-energy extraction. *Mar. Struct.* **2007**, *20*, 185–201.
3. Falcão, A.F. Wave energy utilization: A review of the technologies. *Renew. Sustain. Energy Rev.* **2010**, *14*, 899–918.
4. Budal, K.; Falnes, J. A resonant point absorber of ocean-wave power. *Nature* **1975**, *256*, 478–479.
5. Clément, A.; McCullen, P.; Falcão, A.; Fiorentino, A.; Gardner, F.; Hammarlund, K.; Lemonis, G.; Lewis, T.; Nielsen, K.; Petroncini, S.; *et al.* Wave energy in Europe: Current status and perspectives. *Renew. Sustain. Energy Rev.* **2002**, *6*, 405–431.
6. Leijon, M.; Danielsson, O.; Eriksson, M.; Thorburn, K.; Bernhoff, H.; Isberg, J.; Sundberg, J.; Ivanova, I.; Sjöstedt, E.; Ågren, O.; *et al.* An electrical approach to wave energy conversion. *Renew. Energy* **2006**, *31*, 1309–1319.
7. Thorburn, K.; Bernhoff, H.; Leijon, M. Wave energy transmission system concepts for linear generator arrays. *Ocean. Eng.* **2004**, *31*, 1339–1349.
8. Leijon, M.; Bernhoff, H.; Agren, O.; Isberg, J.; Sundberg, J.; Berg, M.; Karlsson, K.E.; Wolfbrandt, A. Multiphysics simulation of wave energy to electric energy conversion by permanent magnet linear generator. *IEEE Trans. Energy Convers.* **2005**, *20*, 219–224.
9. Eriksson, M.; Waters, R.; Svensson, O.; Isberg, J.; Leijon, M. Wave power absorption: Experiments in open sea and simulation. *J. Appl. Phys.* **2007**, *102*, doi:10.1063/1.2801002.
10. Waters, R.; Stålberg, M.; Danielsson, O.; Svensson, O.; Gustafsson, S.; Strömstedt, E.; Eriksson, M.; Sundberg, J.; Leijon, M. Experimental results from sea trials of an offshore wave energy system. *Appl. Phys. Lett.* **2007**, *90*, doi:10.1063/1.2432168.
11. Lejerskog, E.; Boström, C.; Hai, L.; Waters, R.; Leijon, M. Experimental results on power absorption from a wave energy converter at the Lysekil wave energy research site. *Renew. Energy* **2015**, *77*, 9–14.
12. Stålberg, M.; Waters, R.; Danielsson, O.; Leijon, M. Influence of Generator Damping on Peak Power and Variance of Power for a Direct Drive Wave Energy Converter. *J. Offshore Mech. Arct. Eng.* **2008**, *130*, doi:10.1115/1.2905032.
13. Engström, J.; Kurupath, V.; Isberg, J.; Leijon, M. A resonant two body system for a point absorbing wave energy converter with direct-driven linear generator. *J. Appl. Phys.* **2011**, *110*, doi:10.1063/1.3664855.
14. Kurupath, V.; Ekström, R.; Leijon, M. Optimal Constant DC Link Voltage Operation of a Wave Energy Converter. *Energies* **2013**, *6*, 1993–2006.
15. Ekström, R.; Ekergård, B.; Leijon, M. Electrical damping of linear generators for wave energy converters—A review. *Renew. Sustain. Energy Rev.* **2015**, *42*, 116–128.
16. Eidsmoen, H. Optimum Control of a Floating Wave-Energy Converter with Restricted Amplitude. *J. Offshore Mech. Arct. Eng.* **1996**, *118*, 96–102.
17. Babarit, A.; Duclos, G.; Clément, A.H. Comparison of latching control strategies for a heaving wave energy device in random sea. *Appl. Ocean. Res.* **2004**, *26*, 227–238.
18. Babarit, A.; Clément, A.H. Optimal latching control of a wave energy device in regular and irregular waves. *Appl. Ocean. Res.* **2006**, *28*, 77–91.
19. Babarit, A.; Guglielmi, M.; Clément, A.H. Declutching control of a wave energy converter. *Ocean. Eng.* **2009**, *36*, 1015–1024.
20. Sheng, W.; Alcorn, R.; Lewis, A. On improving wave energy conversion, part II: Development of latching control technologies. *Renew. Energy* **2015**, *75*, 935–944.

21. Oskamp, J.A.; Özkan-Haller, H.T. Power calculations for a passively tuned point absorber wave energy converter on the Oregon coast. *Renew. Energy* **2012**, *45*, 72–77.
22. Jaén, A.D.L.V.; Andrade, D.E.M.; Santana, A.G. Increasing the efficiency of the passive loading strategy for wave energy conversion. *J. Renew. Sustain. Energy* **2013**, *5*, doi:10.1063/1.4824416.
23. Abraham, E.; Kerrigan, E.C. Optimal Active Control and Optimization of a Wave Energy Converter. *IEEE Trans. Sustain. Energy* **2013**, *4*, 324–332.
24. Shek, J.K.H.; Macpherson, D.E.; Mueller, M.A.; Xiang, J. Reaction force control of a linear electrical generator for direct drive wave energy conversion. *IET Renew. Power Gener.* **2007**, *1*, 17–24.
25. Molinas, M.; Skjervheim, O.; Andreasen, P.; Undeland, T.; Hals, J.; Moan, T.; SØrby, B. Power Electronics as Grid Interface for Actively Controlled Wave Energy Converters. In Proceedings of the International Conference Clean Electric Power 2007 ICCEP 07, Capri, Italy, 21–23 May 2007; pp. 188–195.
26. Korde, U. Control System Applications in Wave Energy Conversion. In Proceedings of the OCEANS 2000 MTSIEEE Conference Exhibition, Providence, RI, USA, 11–14 September 2000; Volume 3, pp. 1817–1824.
27. Hals, J.; Falnes, J.; Moan, T. A Comparison of Selected Strategies for Adaptive Control of Wave Energy Converters. *J. Offshore Mech. Arct. Eng.* **2011**, *133*, doi:10.1115/1.4002735.
28. Bacelli, G.; Ringwood, J.; Gilloteaux, J.C. A Control System for a Self-Reacting Point Absorber Wave Energy Converter Subject to Constraints. In Proceedings of the 18th IFAC World Congress. Milano, Italy, 28 August–2 September 2011; pp. 11387–11392.
29. Bacelli, G.; Ringwood, J. Constrained control of arrays of wave energy devices. *Int. J. Mar. Energy* **2013**, *3–4*, e53–e69.
30. Ekström, R.; Kurupath, V.; Boström, C.; Waters, R.; Leijon, M. Evaluating Constant DC-Link Operation of Wave Energy Converter. *J. Dyn. Syst. Meas. Control.* **2013**, *136*, doi:10.1115/OMAE2012-83339.
31. Wang L.; Engström, J.; Göteman, M.; Isberg, J. Constrained optimal control of a point absorber wave energy converter with linear generator. *J. Renew. Sustain. Energy.* **2015**, submitted.
32. Cargo, C.J.; Hillis, A.J.; Plummer, A.R. Optimisation and control of a hydraulic power take-off unit for a wave energy converter in irregular waves. *Proc. Inst. Mech. Eng. Part J. Power Energy* **2014**, *228*, 462–479.
33. Pierson, W.J.; Moskowitz, L. A proposed spectral form for fully developed wind seas based on the similarity theory of S.A. Kitaigorodskii. *J. Geophys. Res.* **1964**, *69*, 5181–5190.
34. WAMIT. *WAMIT User Manual version 7.0 n.d*; WAMIT: Boston, MA, USA, 2013.
35. Engström, J.; Eriksson, M.; Isberg, J.; Leijon, M. Wave energy converter with enhanced amplitude response at frequencies coinciding with Swedish west coast sea states by use of a supplementary submerged body. *J. Appl. Phys.* **2009**, *106*, doi:10.1063/1.3233656.
36. Kara, F. Time domain prediction of power absorption from ocean waves with latching control. *Renew. Energy* **2010**, *35*, 423–434.